Stacking Efficiency of Diselenadiazolyl π-Dimers. Consequences for Electronic Structure and Transport Properties

J. F. Britten,[1a] O. P. Clements,[1b] A. W. Cordes,[1c] R. C. Haddon,[1d] R. T. Oakley,*[,1b] and J. F. Richardson[1e]

Department of Chemistry, McMaster University, Hamilton, Ontario L8S 4M1 Canada, Department of Chemistry, University of Waterloo, Waterloo, Ontario N2L 3G1 Canada, Department of Chemistry and Biochemistry, University of Arkansas, Fayetteville, Arkansas 72701, Department of Chemistry, University of California, Riverside, California 92521−0403, and Department of Chemistry, University of Louisville, Louisville, Kentucky 40292

Received June 28, 2001

The preparation and crystal structure of 5-cyanofuran-2-[1,2,3,5-diselenadiazolyl], [RCN_2Se_2] (R = 5-cyanofuran), is reported. Crystal data for $C_6H_2ON_3Se_2$: monoclinic, space group $P2_1$, a = 7.1121(7), b= 20.541(2), c =20.923-(2) Å, β = 99.785(1)°, Z = 16. The crystal structure consists of diselenadiazolyl π-dimer stacks running parallel to the x direction; the asymmetric unit consists of four π-dimer units. The dimers are aligned into snakelike ribbons along the y direction, with consecutive dimers linked by head-to-tail CN−Se contacts. Each π-dimer stack is bordered by two out-of-register stacks, but most interstack Se−Se contacts lie outside the van der Waals separation. Along the π-dimer stacks, the intradimer Se−Se distances range from 3.183(10) to 3.294(1) Å, and the interdimer Se−Se distances range from 3.826(1) to 3.945(1) Å. Like other π-dimer stacked diselenadiazolyls, $[C_6H_2ON_3Se_2]_2$ is diamagnetic over the temperature range 4−380K. Variable temperature single-crystal conductivity measurements reveal a room-temperature conductivity near 10^{-5} S cm^{-1} and provide a calculated band gap of 0.72 eV. The structural results and transport properties are interpreted in the light of Extended Hückel band structure calculations.

Introduction

The potential applications of 1,2,3,5-dithiadiazolyl radicals, **1a**, in the design of molecular conductors,[2] magnets,[3] and thin film devices[4] have led to extensive research into the structure/property relationships of these materials.[5] In the solid state, the radicals are usually found as diamagnetic dimers, although dimerization can be inhibited by steric effects.[6] The weak intradimer S−S "bonds" dissociate at elevated temperatures,[6b] but the consequent enhancements in magnetic susceptibility are not associated with a major increase in conductivity, indicating that the liberated spins are not charge carriers. Within a simple band model of electronic structure, these findings can be interpreted in terms of a collapse of intermolecular overlap as the dimers separate into radicals. The consequent bandwidth is insufficient to offset the Coulombic barrier to charge transfer (U), and the materials convert to a Mott insulating rather than metallic state. Conductivity can be enhanced by p type doping, e.g., by oxidation with halogens.[7] As a result of oxidation, the level of band filling is no longer commensurate with dimerization and, more importantly, the value of U, which is a maximum for a half-filled energy band, is reduced. But in the absence of doping, the energetics of charge transfer between neutral dithiadiazolyls limits their utility as conductive materials.

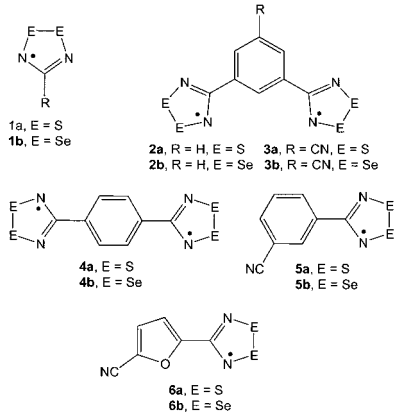

The conductivity of the corresponding selenium based radicals, i.e., 1,2,3,5-diselenadiazolyls **1b**, is significantly better. With one exception,[8] the reported crystal structures consist of cofacial π-dimers, and magnetic measurements indicate much

(1) (a) McMaster University. (b) University of Waterloo. (c) University of Arkansas. (d) University of California. (e) University of Louisville.
(2) (a) Cordes, A. W.; Haddon, R. C.; Oakley, R. T. In *The Chemistry of Inorganic Ring Systems*; R. Steudel, Ed.; Elsevier: Amsterdam, 1992; p. 295. (b) Cordes, A. W.; Haddon, R. C.; Oakley, R. T. *Adv. Mater*. **1994**, *6*, 798.
(3) (a) Banister, A. J.; Bricklebank, N.; Lavender, I.; Rawson, J. M.; Gregory, C. I.; Tanner, B. K.; Clegg, W.; Elsegood, M. R. J.; Palacio, F. *Ang. Chem., Int. Ed. Engl.* **1996**, *35*, 2533. (b) Antorrena, J. E.; Davies, J. E.; Harley, M.; Palacio, F.; Rawson, J. M.; Smith, J. N.; Steiner, A. *Chem. Commun.* **1999**, 1393.
(4) Cordes, A. W.; Haddon, R. C.; MacKinnon, C. D.; Oakley, R. T.; Patenaude, G. W.; Reed, R. W.; Rietveld, T.; Vajda, K. E. *Inorg. Chem*. **1996**, *35*, 7626.
(5) Banister, A. J.; Rawson, J. M. In *The Chemistry of Inorganic Ring Systems*; R. Steudel, Ed.; Elsevier: Amsterdam, 1992; p. 323. (b) Banister, A. J.; Rawson, J. M. *Adv. Heterocycl. Chem*. **1995**, *62*, 137. (c) Torroba, T. *J. Prakt. Chem*. **1999**, *341*, 99.
(6) (a) Barclay, T. M.; Cordes, A. W.; George, N. A.; Haddon, R. C.; Itkis, M. E.; Oakley, R. T. *Chem. Commun*. **1999**, 2269. (b) Beekman, R. A.; Boeré, R. T.; Moock, K. H.; Parvez, M. *Can. J. Chem*. **1998**, *76*, 85.

10.1021/ic010678v CCC: $20.00
Published on Web 11/20/2001

stronger intradimer Se−Se interactions, the compounds are diamagnetic. In several cases, structural and transport property data are available on both sulfur and selenium containing systems, e.g., the bifunctional radicals **2**,[9] **3**,[10] and **4**.[11] The respective pairs (E = S/Se) are all isostructural in the solid state (although there is a second phase[12] known for **2b**). In contrast to the sulfur based compounds, the selenium materials remain essentially diamagnetic to temperatures well above 200°C and exhibit conductivity/temperature profiles characteristic of an intrinsic semiconductor. From an applications viewpoint, these bifunctional materials are, however, not easy to manipulate. Their vaporization requires extreme temperature and vacuum conditions, and sublimation is often accompanied by sample decomposition.

By contrast, purification and crystal growth of monofunctional diselenadiazolyls by vacuum sublimation is relatively straightforward. Several pairs (E = S/Se) have been structurally characterized, but different packing patterns are often observed for the two partners, e.g., **1** (R = H, Ph).[13,14] However, when R = 3-cyanophenyl, i.e., **5**, the packing patterns are identical for E = S and Se,[15] i.e., stacked π-dimers, akin to those observed for **2** and **3**, so correlations of structure and property are possible. In general, the conductivity of monofunctional derivatives is markedly lower than that of bifunctional materials. For example, the room-temperature conductivity σ_{RT} of **5b** is near 10^{-9} S cm^{-1}, while for **2b**,[9] $\sigma_{RT} \approx 10^{-4}$ S cm^{-1}.

While exploring the packing patterns of monofunctional π-dimer stacks, we considered the cyanofuryl derivatives **6**.[16] At the level of lock−and−key parlance, these radicals might be expected to display a similar packing pattern to that exhibited by **5**. X-ray characterization of **6a** confirmed this supposition, but also revealed a much tighter packing of the π-dimers along the stacking direction. At the time, we suspected that if **6b** were to pack with similar efficiency, it should display a relatively high conductivity, comparable to those seen for **2b** and **3b**. However, while preparation and purification of **6b** proved to be a routine task, repeated attempts to determine the crystal structure were thwarted by twinning and superlattice problems. More recently, using X-ray data collected on a CCD instrument and new twinning routines in SHELX software, we have been able to solve the structure and complete the structure/property analysis. Herein, we report the preparation and structural characterization of **6b** and provide a comparative analysis of its electronic structure and conductivity with that of other π-dimer stacks.

Scheme 1

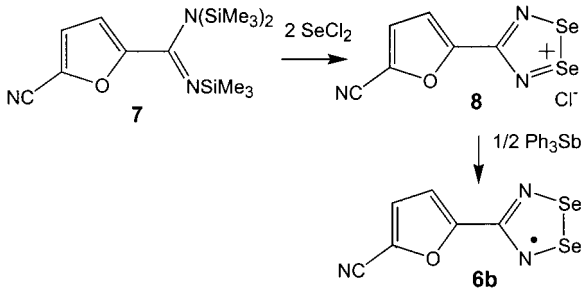

Results and Discussion

Synthesis. Compound **6b** was prepared (Scheme 1) using a variation of the procedure developed for the preparation of **6a**.[16] Accordingly, the cyanofuryl functionalized persilylated amidine **7**, itself prepared by the reaction of 2,5-dicyanofuran with lithium bistrimethylsilylamide, was treated with 2 equiv of $SeCl_2$, which was prepared in situ from Se and $SeCl_4$. The diselenadiazolylium chloride **8** was reduced with triphenylantimony, and the radical **6b** was separated and purified by sublimation in vacuo.

Crystal Structure. Bronze needlelike crystals of **6b** (several were examined) gave a diffraction pattern which appeared to be *C* centered orthorhombic. However, a primitive monoclinic cell of half the volume showed slightly better merging statistics, and $P2_1$ proved to be the correct space group. A routine direct methods solution (SHELXS) clearly showed eight independent molecules, or four dimers, in the asymmetric unit. Full anisotropic refinement converged with R_1 = 7.03%, the Flack parameter = 0.18(3), a high variance for the weak data, and a definite trend of $F_c < F_o$ for the poorly fitting reflections. Refinement with compensation for inversion twinning only improved R_1 to 6.98%, but there was still evidence of further twinning. Addition of a pseudomerohedral twin correction for a two-fold rotation around the *a**, *c** face diagonal (a two-fold axis in the pseudo-orthorhombic cell) cleaned up the refinement and difference map. The refined twin component fractions were 0.15(1), 0.11(1), and 0.06(1) for the rotational, inversion, and inverted rotational contributions, respectively. The final R_1 was 3.15%, and the molecules showed the expected geometry. The unusually high value of $Z' = 8$ independent molecules and the low packing symmetry result from the alternation in intermolecular contacts along *x*, the slight shift of one stack relative to the next (out-of-register stacking) with a period of four stacks along *z*, and the sinusoidal variation of the molecular plane perpendicular to *y*. All of these packing effects result in a reduction of the electronic strain of the solid, as discussed below.

Crystal data for **6b** is presented in Table 1, and a summary of pertinent intramolecular bond lengths, as well as intradimer

(7) Bryan, C. D.; Cordes, A. W.; Haddon, R. C.; Hicks, R. G.; Kennepohl, D. K.; MacKinnon, C. D.; Oakley, R. T.; Palstra, T. T. M.; Perel, A. S.; Scott, S. R.; Schneemeyer, L. F.; Waszczak, J. V. *J. Am. Chem. Soc.* **1994**, *116*, 1205. (b) Bryan, C. D.; Cordes, A. W.; Fleming, R. M.; George, N. A.; Glarum, S. H.; Haddon, R. C.; MacKinnon, C. D.; Oakley, R. T.; Palstra, T. T. M., Perel, A. S.; Schneemeyer, L. F.; Waszczak, J. V. *J. Am. Chem. Soc.* **1995**, *117*, 6880. (c) Cordes, A. W.; George, N. A.; Haddon, R. C.; Kennepohl, D. K.; Oakley, R. T. Palstra, T. T. M.; Reed, R. W. *Chem. Mater.* **1996**, *8*, 2774. (d) Bryan, C. D.; Cordes, A. W.; Goddard, J. D.; Haddon, R. C.; Hicks, R. G.; MacKinnon, C. D.; Mawhinney, R. C.; Oakley, R. T.; Palstra, T. T. M.; Perel, A. S. *J. Am. Chem. Soc.* **1996**, *118*, 330.

(8) Feeder, N.; Less, R. J.; Rawson, J. M.; Oliete, P.; Palacio, F. *Chem. Commun.* **2000**, 2449.

(9) Cordes, A. W.; Haddon, R. C.; Oakley, R. T.; Schneemeyer, L. F.; Waszczak, J. V.; Young, K. M.; Zimmerman, N. M. *J. Am. Chem. Soc.* **1991**, *113*, 582.

(10) Andrews, M. P.; Cordes, A. W.; Douglass, D. C.; Fleming, R. M.; Glarum, S. H.; Haddon, R. C.; Marsh, P.; Oakley, R. T.; Palstra, T. T. M.; Schneemeyer, L. F.; Trucks, G. W.; Tycko, R. R.; Waszczak, J. V.; Warren, W. W.; Young, K. M.; Zimmerman, N. M. *J. Am. Chem. Soc.* **1991**, *113*, 3559.

(11) Cordes, A. W.; Haddon, R. C.; Hicks, R. G.; Kennepohl, D. K.; Oakley, R. T.; Palstra, T. T. M.; Schneemeyer, L. F.; Scott, S. R.; Waszczak, J. V. *Chem. Mater.* **1993**, *5*, 820.

(12) Cordes, A. W.; Haddon, R. C.; Hicks, R. G.; Oakley, R. T.; Palstra, T. T. M.; Schneemeyer, L. F.; Waszczak, J. V. *J. Am. Chem. Soc.* **1992**, *114*, 1729.

(13) Cordes, A. W.; Bryan, C. D.; Davis, W. M.; de Laat, R. H.; Glarum, S. H.; Goddard, J. D.; Haddon, R. C.; Hicks, R. G.; Kennepohl, D. K.; Oakley, R. T.; Scott, S. R.; Westwood, N. P. C. *J. Am. Chem. Soc.* **1993**, *115*, 7232.

(14) (a) Vegas, A.; Peréz-Salazar, A.; Banister, A. J.; Hey, R. G.; *J. Chem. Soc., Dalton Trans.* **1980**, 1812. (b) Del Bel Belluz, P.; Cordes, A. W.; Kristof, E. M.; Kristof, P. V.; Liblong, S. W.; Oakley, R. T. *J. Am. Chem. Soc.* **1989**, *111*, 9276.

(15) Cordes, A. W.; Haddon, R. C.; Hicks, R. G.; Oakley, R. T.; Palstra, T. T. M. *Inorg. Chem.* **1992**, *31*, 1802.

(16) Cordes, A. W.; Chamchoumis, C. M.; Hicks, R. G.; Oakley, R. T.; Young, K. M.; Haddon, R. C. *Can. J. Chem.* **1992**, *70*, 929.

Table 1. Crystal Data for **6b**

formula	$C_6H_2N_3OSe_2$
fw	290.03
a, Å	7.1121(7)
b, Å	20.541(2)
c, Å	20.923(2)
β, deg	99.785(1)
V, Å^3	3012.2(5)
ρ(calcd), g cm^{-3}	2.558
space group	$P2_1$ (No. 4)
Z	16
temp, K	298(2)
μ, mm^{-1}	9.764
λ, Å	0.71073
data/restraints/parameters	12838/1/868
solution method	direct methods
R, R_w	0.0315, 0.0764 (on F^2)[a]

[a] $R = [\sum||F_o| - |F_c||]/[\sum|F_o|]$; $R_w = \{[\sum w||F_o|^2 - |F_c|^2|^2]/[\sum(w|F_o|^4)]\}^{1/2}$.

Table 2. Selected Intramolecular Distances and Intra- and Interdimer Se−Se Distances in **6b** (in Å)

Intramolecular

	Se−Se	Se−N	N−C
range	2.310(1)−2.316(1)	1.760(7)−1.806(7)	1.300(10)−1.359(10)
mean	2.313	1.780	1.326

Intradimer

	Se	Se2
A−B	3.285(1)	3.202(1)
E−F	3.284(1)	3.206(1)
C−D	3.285(1)	3.189(1)
G−H	3.294(1)	3.183(1)

Interdimer

	Se1	Se2
A−B	3.837(1)	3.917(1)
E−F	3.842(1)	3.916(1)
C−D	3.852(1)	3.942(1)
G−H	3.826(1)	3.945(1)

Intrastack

A−E	3.980(1)	B−E	4.096(1)
A−F	3.909(1)	B−F	4.030(1)
C−G	4.000(1)	D−G	4.106(1)
C−H	3.963(1)	D−H	3.918(1)
A−G	3.659(1)	B−G	3.882(1)
A−H	3.663(1)	B−H	3.893(1)
C−E	3.898(1)	D−E	3.760(1)
C−F	3.7729(1)	D−F	3.665(1)

Se−Se and interdimer Se−Se contacts is provided in Table 2. An ORTEP drawing[17] of the asymmetric unit, showing atom numbering, is shown in Figure 1. The packing motif, viewed down the *x* direction (Figure 2), is similar to that observed for **5a/b** and **6a**, with the dimers forming snakelike ribbons in which neighboring molecules are linked in a head-to-tail fashion by E−NC (E = S, Se) contacts. The role of these secondary bonding interactions[18] as structure making "supramolecular synthons"[19] is well recognized.[10,15,16,20] Other donor−acceptor combinations, e.g., secondary F−Se contacts, have recently been shown to have a similar structure-influencing role.[21]

In contrast to **5a/b** and **6a**, there are four dimers (labeled as A/B, C/D, E/F, and G/H) in the asymmetric unit. The packing

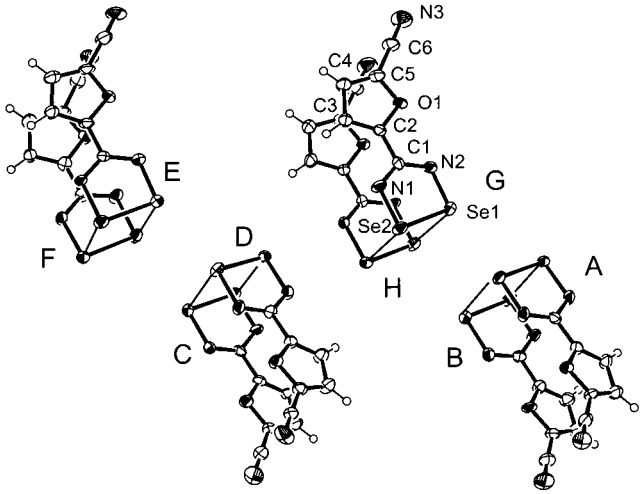

Figure 1. ORTEP drawing (50% probability ellipsoids) of the asymmetric unit of **6b**. Atom numbering of all rings (A−H) follows that shown for ring G.

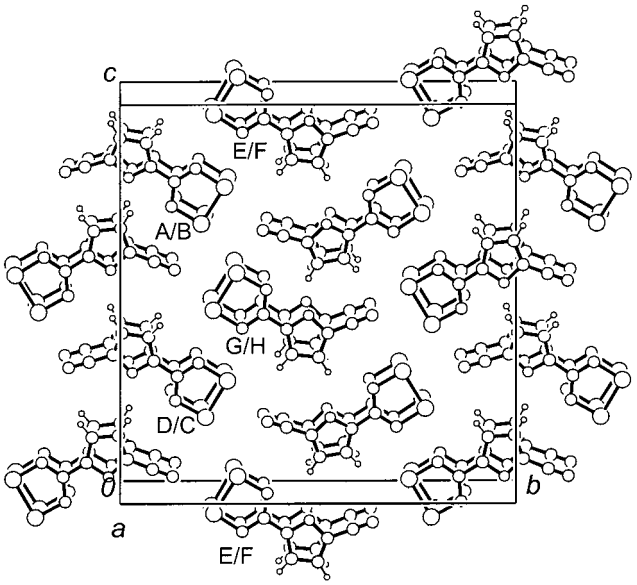

Figure 2. Packing of dimers in the unit cell of **6b** viewed parallel to the *x* axis.

of the rings gives rise to two types of local environments for the dimers. The side-on or partial dovetailed arrangement, e.g., A/B with E/F, is a very common feature in dithia- and diselenadiazolyl structures, as it maximizes electrostatic interactions between adjacent rings. The more head-to-head interaction, e.g., A/B with G/H, is symptomatic of the curvature of the molecular ribbons, which prevents the ideal dovetailed arrangement found, for example, in 4-$NCC_6H_4CN_2E_2$.

Viewed perpendicular to the stacking direction, the dimers form π-stacked arrays, with neighboring stacks aligned approximately out-of register (Figure 3). This arrangement gives rise to numerous Se−Se interactions, both within and between the stacks. However, relatively few of these contacts lie significantly inside the standard Se−Se van der Waals contact of 3.8 Å.[22] Of more note, in comparison to the structure of **5b**, and also the band structure calculations and conductivity measurements which follow, are the intra- and interdimer contacts along the

(17) ORTEP-3 for Windows: Farrugia, L. J. *J. Appl. Crystallogr.* **30**, 565 1997.
(18) Vargas-Baca, I.; Chivers, T. *Main Group Chem. News*. **1999**, *7*, 4, 6.
(19) Reddy, D. S.; Ovechinnikov, Shiskin, O. V.; Struchkov, Y. T.; Desiraju, *G. R. J. Am. Chem. Soc*. **1996**, *118*, 4085.
(20) Davis, W. M.; Hicks, R. G.; Oakley, R. T.; Zhao, B.; Taylor, N. J. *Can. J. Chem.* **1993**, *71*, 180.
(21) Beer, L.; Cordes, A. W.; Myles, D. J. T.; Oakley, R. T.; Taylor, N. J. *CrystEngComm* **2000**, 20.
(22) Bondi, A. *J. Phys. Chem.* **1964**, *68*, 441.

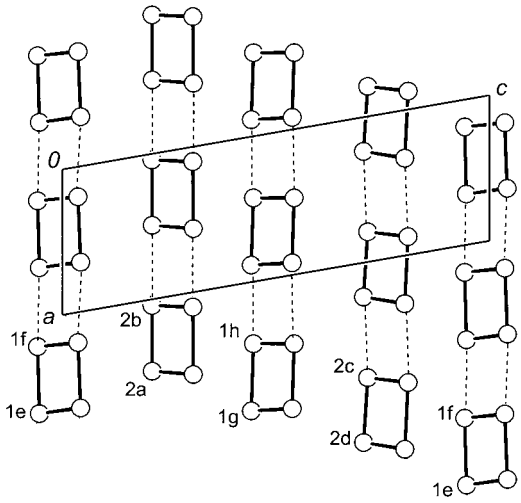

Figure 3. Out-of-register stacking of dimer units in **6b**. Only the Se atoms (with atom numbering) are shown.

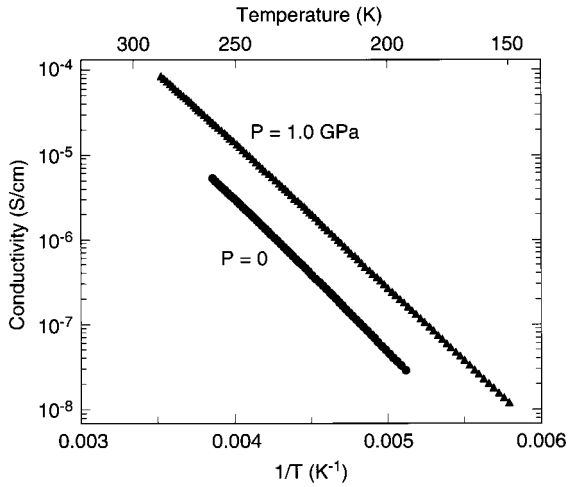

Figure 4. Log plots of the conductivity σ of **6b** as a function of inverse temperature with and without applied pressure.

stacks; the mean values are, respectively, 3.241 and 3.885 Å. By contrast, the corresponding mean intra- and interdimer distances in **5b** are 3.27 and 4.15 Å. Indeed, the interdimer contacts of this monofunctional radical are *closer* than those seen in the bifunctional radicals **2b** (4.014 Å) and **3b** (3.91 Å). The contraction in the dimer separation in **6b** (and its sulfur analogue **6a**) is, we believe, a consequence of the more efficient layering of the dimer ribbons occasioned by the smaller size of the cyanofuryl group relative to that of the cyanophenyl group. Essentially, by reducing the steric bulk of the "structure making" 4-substituent, a much tighter packing of the dimers can be induced. However, this more efficient stacking of dimers along *x* does little to improve lateral interactions, as a result of which, the structure remains highly one dimensional (see below).

Conductivity Measurements. In accord with previous findings on π-stacked diselenadiazolyl dimers, magnetic susceptibilty measurements on **6b** confirm that it is diamagnetic from 4−380 K, with an observed diamagnetism of -180×10^{-6} emu mol^{-1}. Four probe single-crystal conductivity measurements on **6b** reveal a room-temperature conductivity $\sigma_{RT} \approx 0.10^{-5}$ S cm^{-1}, a value about 4 orders of magnitude greater than that found for **5b**. Application of 1 GPa pressure leads to an increase[9] in conductivity of nearly an order of magnitude. Log plots (with and without applied pressure) of the single-crystal conductivity of **6b** as a function of temperature are provided in Figure 4. If,

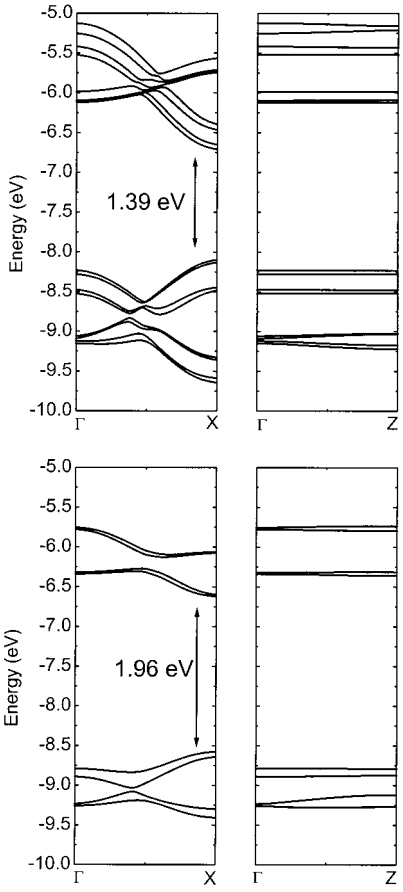

Figure 5. Dispersion of valence and conduction COs of **6b** (above) and **5b** (below). $\Gamma = (0, 0)$, $X = (a^*/2, 0)$, $Z = (0, c^*/2)$.

as before, the material is treated as an intrinsic semiconductor, we obtain values for the activation energy E_g of 0.72 eV. This value can be compared with that of 0.55 eV for **2b**[9] and 0.64 eV for **3b**.[10]

Band Electronic Structure Calculations. To probe the extent of electronic interactions within and between the π-dimer stacks of **6b**, we performed Extended Hückel Theory (EHT) band calculations on a model structure in which the cyanofuryl group was replaced with a simple hydrogen ligand. All other atomic coordinates were taken from the crystal structure. Only interactions along and lateral to the stacking directions were considered. The results are expressed in the form of a two-dimensional ($\Gamma \rightarrow X$ and $\Gamma \rightarrow Z$) crystal orbital (CO) dispersion diagram (Figure 5) for the valence and conduction bands. These bands are comprised of the COs arising from the two highest occupied and two lowest unoccupied molecular orbitals of the four dimers.[23] Also shown are the corresponding 2-D dispersion curves for **5b**. In this latter case, only the COs arising from the highest occupied and lowest unoccupied molecular orbitals are included.

Inspection of the dispersion curves for both **5b** and **6b** indicate that both structures are highly one dimensional. Dispersion lateral to the stacks ($\Gamma \rightarrow Z$) is almost flat, as expected from the structural analysis provided earlier (the absence of lateral Se—Se contacts inside the van der Waals separation). By contrast, but also in keeping with the structural data, dispersion along the stacking direction is far more substantial for **6b** than for **5b**; indeed, in **6b** along-the-stack dispersion ($\Gamma \rightarrow X$) is the

(23) There are several avoided crossings along *X*; these arise from strong mixing of the COs associated with the π orbitals of the molecular units.

Table 3. Room Temperature Conductivity σ_{RT} (S cm^{-1}) and Measured and Calculated (EHT) Band Gaps[a] E_g (eV) of Diselenadiazolyl Radical Dimers

compound	σ_{RT}	E_g (meas.)	E_g (calc.)
2b	10^{-4}	0.55	0.88/0.93[b]
3b	10^{-7}	0.64	1.52
5b	10^{-9}	–	1.96
6b	10^{-5}	0.72	1.39

[a] Band gaps estimated from dispersion curve data. [b] The two values are taken from calculations on pinwheel stacks about the 4_1 and $\bar{4}$ axes.

largest ever observed in a monofunctional diselenadiazolyl dimer stack. As a result of this enhanced spreading of both the valence and conduction bands, the band gap predicted for **6b** is dramatically reduced relative to those calculated for other monofunctional systems, e.g., **5b**, and similar to that encountered for bifunctional radical **3b**[24] (Table 3). Only in the case of **2b**, where a more two-dimensional structure is observed, is the band gap substantially smaller.[25]

Summary and Conclusions

By suitable choice of 4-substituents, 1,2,3,5-diselenadiazolyl radicals can be induced to crystallize as π-dimer stacks, affording semiconductive materials with tunable band gaps. The enhanced conductivity of the cyanofuryl derivative **6b** relative to that of the 3-cyanophenyl compound **5b** can be traced to a more efficient packing allowed by the cyanofuryl ligand. This "chemical pressure" leads to a closer separation of dimers along the π-stack and, hence, a greater bandwidth for both the valence and conduction bands (the HOMO and LUMO of the dimers). The band gap found for **6b** compares favorably with those found for the bifunctional materials **2b** and **3b**. The importance of this result lies in the implication that thermally stable and relatively volatile (easily sublimable) low band gap semiconductive materials based on monofunctional diselenadiazoyls can be designed.

Experimental Section

General Procedures and Starting Materials. Furan-2,5-dimethanol, selenium powder, triphenylantimony (Aldrich), and chlorine (Matheson) were obtained commercially and used as received. Selenium tetrachloride[26] was prepared using standard literature procedures, and lithium bis(trimethylsilyl)amide (Aldrich) was converted into its etherate[27] to facilitate amidine synthesis. Acetonitrile (Fisher HPLC grade) was purified by distillation from P_2O_5. Dicyanofuran was prepared by the oxidation of furan-3,5-dimethanol to the corresponding dialdehyde[28] and conversion of the latter to the dioxime;[29] subsequent dehydration with acetic acid afforded the desired dinitrile.[30] Fractional sublimations were performed in an ATS series 3210 three-zone tube furnace, mounted horizontally, and linked to a series 1400 temperature control system. Mass spectra were recorded on a Kratos MS890 mass spectrometer. Elemental analyses were performed by MHW Laboratories, Phoenix, AZ. Infrared spectra were recorded (at 2 cm^{-1} resolution on Nujol mulls) on a Nicolet 20SX/C FTIR spectrometer.

Synthesis of 5-Cyanfuran-2-[1,2,3,5-diselenadiazolyl], 6b. Solid *N*,*N*,*N*′-tris(trimethylsilyl)-5-cyano-2-furylamidine[16] (1.76 g, 5.0 mmol) was added to a solution of $SeCl_2$ (made from $SeCl_4$ (1.10 g, 5.0 mmol)) and Se powder (0.39 g, 5.0 mmol) in 50 mL of acetonitrile. The mixture was refluxed for 1 h, cooled to room temperature, and the resulting bright, brick red solid was filtered off, rinsed with acetonitrile (three 20 mL portions), and dried in vacuo. The crude diselenadiazolylium chloride was slurried in 50 mL of acetonitrile and treated with solid triphenylantimony (0.91 g, 2.6 mmol). The dark mixture was gently refluxed for 1 h and then cooled to room temperature. A dark brown solid was filtered off, rinsed with acetonitrile, and pumped to dryness. The crude diselenadiazolyl radical was sublimed at 170°C/10^{-2} Torr to afford pure **6b** as lustrous bronze needles, yield 1.00 g (68%). dec > 310 °C. IR spectrum (2000−250 cm^{-1}): 1460 (s), 1377 (s), 1310 (s), 1223 (w), 1214 (m), 1140 (m), 1021 (s), 972 (w), 963 (s), 889 (w), 880 (w), 828 (m), 816 (w), 805 (s), 741 (s), 700 (m), 688 (m), 664 (s), 593 (w), 583 (w), 556 (w), 467 (m), 421 (s), 415 (s), 300 (s) cm^{-1}; ν(CN) 2228 cm^{-1}. Mass spectrum: *m*/*e* 292 (M^+, 85%), 196 ($(M - NS)^+$, 6%), 174 (Se_2N^+, 94%), 160 (Se_2^+, 72%), 135 (?, 32%), 118 ($(NC(C_4H_2O)CN)^+$, 55%), 94 (SeN^+, 100%). Anal. Calcd for $C_6H_2N_3OSe_2$: C, 24.95; H, 0.70; N, 14.49%. Found: C, 25.00; H, 0.55; N, 14.41%.

X-ray Measurements. A sample of **6b** was glued to a glass fiber, centered on a Bruker P4/CCD diffractometer, and irradiated using 11.25 kW X-rays from a Bruker Mo rotating anode generator. The final diffraction data set, consisting of 28358 reflections (R_{int} = 2.98%, 12857 unique (for Laue symmetry 2); coverage to 0.77 Å = 99%, redundancy = 3.9 (for 2/m symmetry)) was measured at 298 K using narrow frame (0.36°) scanning in Bruker's SMART program and integrated using Bruker's SAINT software. SADABS was used for the absorption correction.[31]

Transport Property Measurements. The magnetic susceptibility of **6b** was measured using the Faraday technique; details of the apparatus have been previously described.[32] Four probe conductivity measurements on **6b** were performed with a Keithley 236 unit.

Electronic Structure Calculations. Molecular and band electronic structure calculations were performed with the EHMACC suite of programs,[33] using the parameters discussed previously.[34] The off-diagonal elements of the Hamiltonian matrix were calculated with the standard weighting formula.[35] Atomic positions were taken from the crystallographic data for **5b** and **6b**.

Acknowledgment. We thank the Natural Science and Engineering Research Council of Canada and the State of Arkansas for financial support. We thank Dr. Charles Campana of Bruker AXS Systems Inc. for useful discussions.

Supporting Information Available: An X-ray crystallographic file in CIF format. This material is available free of charge via the Internet at http://pubs.acs.org.

IC010678V

(24) For consistency, all the band gap estimates reported in Table 3 refer to values taken from dispersion curve data, rather than from a density of states analysis, as used in the earlier reports on **2b** and **3b**.
(25) The calculations on **2b** were performed on partial rather than full structures, using four-column clusters about the 4_1 and 4 axes.
(26) Brauer, G. *Handbook of Preparative Inorganic Chemistry*; Academic Press: New York, 1963; Vol. 1, p 423.
(27) Boeré, R. T.; Oakley, R. T. and Reed, R. W. *J. Organomet. Chem.* **1987**, *331*, 161.
(28) Oleinik, A. F.; Yu Novitskii, *Zh. Org. Chim.* **1970**, *6*, 2632.
(29) El Hajj, T.; Masroua, A.; Martin, J.-C.; Descotes, G. *Bull. Soc. Chim. Fr.* **1987**, 855.
(30) Morikiwa, S.; Teratake, S. *Jpn. Kohai Tokkyo Koho*, 79, 19, 963. Morikiwa, S.; Teratake, S. *Chem. Abstr*. **1979**, *91*, 39301c.
(31) Sheldrick, G. M. *SADABS*; University of Göttingen: Germany, 2000.
(32) (a) DiSalvo, F. J.; Waszczak, J. V. *Phys. Rev.* **1981**, *B23*, 457. (b) DiSalvo, F. J.; Menth, A.; Waszczak, J. V. *Phys. Rev.* **1972**, *B6*, 4574.
(33) EHMACC, Quantum Chemistry Program Exchange, program number 571.
(34) Basch, H.; Viste, A.; Gray, H. B. *Theor. Chim. Acta* **1965**, *3*, 458.
(35) Ammeter, J. H.; Burghi, H. B.; Thibeault, J. C.; Hoffmann, R. *J. Am. Chem. Soc.* **1978**, *100*, 3686.